

# Synergistic effect of rubber powder and nano-silica on pore structure and frost resistance of concrete

Received: 5 September 2025

Accepted: 13 January 2026

Published online: 03 March 2026

Cite this article as: Feng L., Cao H., Shi X. *et al.* Synergistic effect of rubber powder and nano-silica on pore structure and frost resistance of concrete. *Sci Rep* (2026). <https://doi.org/10.1038/s41598-026-36480-8>

Ling-Yun Feng, Hong-Liang Cao, Xin-Wei Shi & Da-Hui Wang

We are providing an unedited version of this manuscript to give early access to its findings. Before final publication, the manuscript will undergo further editing. Please note there may be errors present which affect the content, and all legal disclaimers apply.

If this paper is publishing under a Transparent Peer Review model then Peer Review reports will publish with the final article.

# **Synergistic effect of rubber powder and nano-silica on pore structure and frost resistance of concrete**

Ling-Yun Feng<sup>1</sup>, Hong-Liang Cao<sup>2\*</sup>, Xin-Wei Shi<sup>2</sup>, Da-Hui Wang<sup>2</sup>

<sup>1</sup> College of Geosciences and Engineering, North China University of Water Resources and Electric Power, Zhengzhou 450046, China.

Email: fenglingyun@ncwu.edu.cn

<sup>2</sup> Henan Water Science and Technology Application Center, Henan Provincial Key Laboratory of Water Conservancy Engineering Safety Technology, Zhengzhou 450003, China.

\* Corresponding author Email: 155298967@qq.com

**Abstract:** The effectiveness of air-entraining agents in enhancing the frost resistance of concrete is significantly reduced under low-pressure conditions, such as those found in plateau and alpine regions, leading to severe freeze-thaw damage. To address this challenge, this study investigates the use of rubber powder as a compensatory material for air-entraining agents, introducing “solid pores” to replace traditional air voids. The combined effect of rubber powder and nano-silica was evaluated through macroscopic performance tests and microstructural analyses, focusing on the evolution of pore structure parameters and frost resistance during freeze-thaw cycles. The results show that rubber powder increases the air content and optimizes the pore structure, with “solid pores” accounting for an increasing proportion of total air content as the dosage rises. The addition of nano-silica further refines the pore size distribution by reducing the proportion of larger pores and stabilizing the bubble spacing coefficient. Concrete incorporating both rubber powder and nano-silica exhibits significantly improved frost resistance, with only a slight reduction in compressive strength

compared to ordinary concrete. These findings demonstrate that the synergistic use of rubber powder and nano-silica effectively compensates for the diminished performance of air-entraining agents under low-pressure conditions, offering a practical approach to enhancing the freeze-thaw durability of concrete in cold, high-altitude environments.

**Keywords:** "Solid pores"; Rubber powder; Nano-silica; Pore structure; Frost resistance

## 1. Introduction

Freeze-thaw durability is a critical property for concrete used in water conservancy engineering structures, as freeze-thaw damage can severely compromise structural integrity and lead to a loss of load-bearing capacity well before the end of the design life. For example, at the Chalong Hydropower Station in the Nagchu region of Tibet, the temperature fluctuates above and below freezing 187 times per year, with a freezing depth of approximately 1.0 m. Concrete spalling and detachment are frequently observed on the surface of the spillway's bottom plate, with reinforcement exposed to depths of 8-15 cm<sup>1</sup>, which also leads to the exposure of water stoppers.

The inherent porosity and hydrophilicity of concrete enable external water to infiltrate its micropores through capillary action<sup>2</sup>, increasing its degree of saturation<sup>3</sup>. In low-temperature environments, a portion of the free water within the pore structure freezes, causing volumetric expansion. This expansion generates hydrostatic<sup>4</sup>, osmotic<sup>5</sup>, and crystallization pressure<sup>6</sup>, which together widen primary cracks and form secondary cracks within the cement matrix and at the matrix-aggregate interface. The

propagation of these cracks, along with ongoing freeze-thaw cycles, further deteriorates the concrete. Conversely, if excess water rapidly migrates into adjacent pores during freezing, the resulting stress is alleviated, thereby mitigating freeze-thaw damage. Optimizing the pore structure—for example, by ensuring pore diameters do not exceed  $350\ \mu\text{m}$  <sup>7</sup> and bubble spacing remains below  $250\ \mu\text{m}$  <sup>8, 9</sup>—can significantly enhance the freeze-thaw durability of hydraulic concrete in both freshwater and saltwater environments. Introducing fine air voids to achieve these pore structure parameters is therefore considered one of the most effective strategies for improving freeze-thaw resistance.

Air-entraining agents are currently regarded as one of the most effective means to enhance the frost durability of concrete structures in water conservancy projects. However, in high-altitude and cold regions (such as Tibet), reduced air pressure and lower oxygen levels significantly impair the foaming capacity of air-entraining agents. This leads to decreased bubble stability and a marked increase in the initial average bubble diameter, resulting in a deteriorated pore structure and substantially reduced frost durability in air-entrained concrete. Studies have shown that the foaming ability of single-component air-entraining agents—such as sulfonates, saponins, and polyethers—decreases by 30.1%, 28.1%, and 22.0%, respectively <sup>10</sup>. Additionally, the bubble diameter produced by fatty alcohol polyoxyethylene ether sodium sulfate and alkyl glycosides increases by 81% and 72%, respectively <sup>11</sup>. Although researchers have explored the development and selection of composite air-entraining agents, interactions among different types can complicate practical application and hinder the realization of desired synergistic effects <sup>12</sup>.

Beyond air-entrained concrete, various new types of high frost-

resistant concrete have been proposed. Among these, rubber concrete has attracted considerable attention due to its environmental and economic benefits from waste tire recycling. Current research indicates that rubber particles exhibit effects similar to those of air-entraining agents. For example, Yang et al. 13 reported that incorporating 15% rubber particles of 5-8 mesh, 30-40 mesh, and 60-80 mesh sizes increased the air content of concrete by 15.8%, 30.4%, and 40.7%, respectively. Yu et al. 14 found that both the particle size and dosage of rubber particles influence the porosity of cement mortar, with smaller particles producing more pores, particularly increasing the number of 1000 nm pores. Grinys et al. 15 demonstrated that an appropriate dosage of rubber powder with a particle size of 0-1 mm provides a freezing resistance effect comparable to that of air-entraining agents. In concrete, rubber particles function as "solid pores" 16 and can also introduce beneficial air pores 17. These pores create space for ice expansion and facilitate water migration within the concrete, thereby reducing freeze-thaw damage 18, 19 and significantly enhancing frost resistance. Studies by Pham 20 and Medine 21 have confirmed that rubber materials improve the frost resistance of concrete, with rubberized concrete exhibiting superior freeze-thaw durability even after five years compared to conventional concrete.

However, the pores introduced by rubber particles are not always advantageous. Pham et al. 20 demonstrated that cracks and interconnected pores resulting from incomplete bonding between organic rubber particles and the inorganic cement matrix are highly detrimental to the frost resistance of hydraulic concrete. Furthermore, rubber particles also reduce the compressive strength of concrete. Experimental data indicate that the compressive strength of concrete decreases linearly with increasing rubber

particle content<sup>22, 23</sup>. To mitigate the formation of harmful pores introduced by rubber particles and to enhance both the strength and frost resistance of concrete, the incorporation of nano-silica has proven to be an effective and practical approach. Nano- SiO<sub>2</sub> exhibits strong pozzolanic activity and a micro-aggregate filling effect, which accelerates cement hydration and fills capillary pores within the cement matrix. This process significantly reduces structural defects in the hardened paste and improves both compactness and strength<sup>24, 25</sup>, resulting in lower water retention and increased compressive strength and frost resistance. Mohit Kansotiya et al.<sup>26</sup> investigated the effects of nano-silica and rubber particles on the physical and durability properties of concrete. The test results show that the combination of 5% rubber particles and 3% nano-silica has the best effect. It reduces the plasticity of the concrete by 20.95%, lowers the density by 4.94%, enhances the acid resistance, and decreases the moisture absorption rate by 3.49%. The reinforcing effect of nano-silica on concrete has also been verified in other studies<sup>27, 28</sup>. However, there are not many studies on the synergistic effect of rubber particles and nano-silica on the freeze resistance of concrete. Jicun Shi et al.<sup>29</sup> replaced sand with 5%, 7.5%, and 10% of silane-modified rubber (SR) based on the mass of cement, and replaced cement with 1%, 3%, and 5% of nano-silica based on the mass of cement. The freeze-thaw resistance of concrete mixtures containing SR and NS was studied using the response surface methodology. The effects of silane-modified rubber and nano-silica on the microstructure and freeze-thaw resistance of concrete were analyzed. The experimental results showed that the combination of SR and NS exhibited a synergistic effect, resulting in a more uniform distribution of pores in the concrete. However, the pore structure studied in this document is a genuine pore structure, and it does not

include the "solid pores" filled with rubber particles. Therefore, the influence of the rubber particles in the body of the material on the concrete is still manifested in the macroscopic properties rather than the pore structure. In fact, the influence of rubber particles on the freeze resistance of concrete can be understood at the microscopic level as "solid pores".

Given the close relationship between freeze-thaw damage and the pore structure of concrete, this study proposes using rubber powder to compensate for the diminished effectiveness of air-entraining agents under low air pressure conditions. By replacing air pores with "solid pores" and coupling rubber powder with nano-silica, the approach aims to reduce harmful pores and increase beneficial ones. The synergistic "air-entraining" effect of rubber powder and the "reinforcing" effect of nano-silica are leveraged to minimize harmful air voids and maximize solid pore formation. To address the severe freeze-thaw damage experienced by concrete in cold, low-pressure environments, this study combines macro-scale performance testing with microstructural analysis to investigate the evolution of concrete pore structure parameters after freeze-thaw cycles under the combined influence of rubber powder and nano-silica, and to evaluate their effects on frost resistance.

## **2. Experimental program**

### **2.1 Materials**

The materials used in this study comprised urban tap water, P.O 42.5 ordinary silicate cement (The properties of the cement are shown in Table 1.), continuously graded limestone crushed stone with a particle size of 5-20 mm, river sand with a particle size less than 4.75 mm (fineness modulus of 3.0 and apparent density of 2,680 kg/m<sup>3</sup>, the particle gradation curve is shown in Fig. 1.), rubber

powder with a particle size of 60 mesh (250  $\mu\text{m}$ ) and an apparent density of 1,119  $\text{kg/m}^3$ , and hydrophobic nano-silica. The rubber powder is used without any modification treatment. In fact, the particle size of rubber powder is very small, and the surface modification treatment has a relatively minor impact on the bonding interface between rubber powder and cement stone. Due to the extremely small particle size of rubber powder and nano-silica, they tend to form clumps in the concrete. Therefore, during the concrete mixing process, the rubber powder and nano-silica should be thoroughly mixed and stirred with the dry materials such as cement, coarse aggregates and fine aggregates (dry mixing for about 2 min), and then water should be added and the mixture should be further mixed.

**Table 1 Properties of cement**

<b>cement type</b>	<b>loss on ignition</b>	<b>magnesium oxide</b>	<b>sulfur trioxide</b>	<b>fineness</b>	<b>setting time</b>	<b>Stability (Boiling Test Method)</b>
	Not more than	Not exceeding	Not exceeding	Not exceeding	prehardening	final set
Ordinary Portland cement	5.0	5.0	3.5	10.0	45	10 up to standard

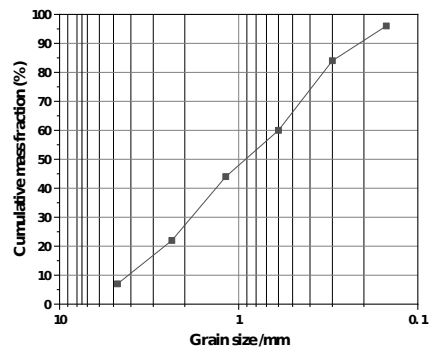


**Fig. 1 Grading curves of the river sand.**

## 2.2 Concrete mix proportions

The concrete mix proportions are presented in [Table 2](#). Group P represents the normal concrete mix. Groups XJ5, XJ10, and XJ20 are derived from Group P by replacing river sand with rubber powder at 5%, 10%, and 15% of equal volume, respectively. Groups GXJ5 and GXJ10 are further modified from Group XJ6, with nano-silica added at 5% and 10% of the cement mass, respectively. **According to relevant research, the maximum amount of rubber powder that can enhance the freeze resistance of concrete is 10% - 15% of the volume of sand replaced. Beyond this range, the rubber concrete will experience a loss in strength and thus its freeze resistance will decrease. Therefore, the maximum amount of rubber powder used in this study is set at 15%. The enhancement effect of nano-silica on the physical and mechanical properties of concrete is not simply proportional to the amount of addition; rather, there exists an optimal value. Beyond this optimal value, the enhancement effect of nano-silica will basically no longer increase. The optimal value as shown by some studies is 5% of the cement quality, while others indicate it to be 10%. Therefore, in this paper, the nano-silica content is set at 5% and 10%.**

**Table 2 Test concrete mixes**

No.	Water	Cement	Coarse aggregate	Fine aggregate	Rubber powder	Nano SiO <sub>2</sub>
P	200	400	1100	700	0	0
XJ5	200	400	1100	665	15	0
XJ10	200	400	1100	630	30	0
XJ15	200	400	1100	595	45	0
GXJ5	200	400	1100	630	30	20
GXJ10	200	400	1100	630	30	40

### 2.3 Pore structure analysis

The pore structure of concrete was evaluated according to the "Test code for hydraulic concrete" (SL/T352-2020) using the linear conductor method. The HYT-QP concrete pore structure parameter analyzer was employed to measure the pore content, average pore size, pore spacing coefficient, and other relevant parameters after each freeze-thaw cycle, as illustrated in Fig. 2. The parameters regarding the concrete pore structure obtained through the wire method describe the actual state of the pores, and are not the "solid pores" filled by the rubber powder. In rubber concrete, "solid pores" refer to the rubber particles themselves and the space they occupy. This concept was proposed to indicate that the effect of rubber particles on the compressive strength of concrete is equivalent to that of real pores. Some scholars also call it "defects" in concrete. The volume content of the "solid pores" is defined in this paper as the ratio of the volume of the rubber particles to the volume of the concrete. The pore diameter of the "solid pores" is taken as the average particle size of the rubber particles.



**Fig. 2 Concrete pore structure test specimen**

## 2.4 Rapid freeze-thaw testing

The rapid freeze-thaw test was conducted in accordance with the “Test code for hydraulic concrete” (SL/T352-2020) [30](#). A concrete rapid freeze-thaw instrument was used, and the number of freeze-thaw cycles was set at 0, 20, 40, 60, 80, and 100 cycles. Concrete specimens were prepared as 100 mm × 100 mm × 100 mm cubes, with three specimens tested for each freeze-thaw cycle group ([Fig. 3](#)).

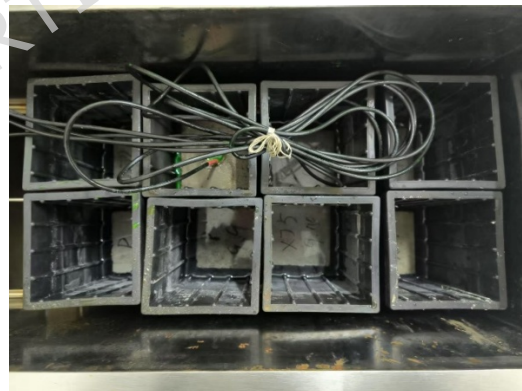


**Fig. 3 Rapid freeze-thaw test of concrete**

## 2.5 Compressive strength testing

The compressive strength of concrete was tested following the “Test code for hydraulic concrete” (SL/T352-2020) [30](#). A microcomputer-controlled electro-hydraulic universal testing

machine was used to test 100 mm × 100 mm × 100 mm cube specimens (Fig. 4). After each designated number of freeze-thaw cycles, the compressive strength test was performed. For each cycle group, three specimens were tested, and the average value was recorded as the compressive strength for that group.

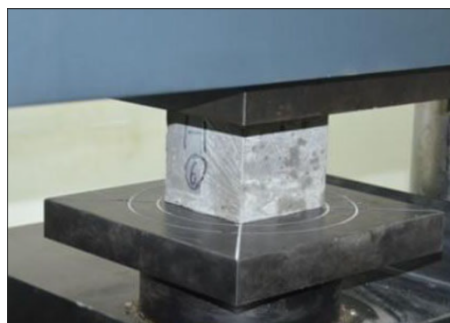


**Fig. 4 concrete compressive strength test**

### **3. Initial pore structure characteristics**

#### **3.1 Influence of rubber powder on pore structure**

The primary effect of rubber powder on concrete is a significant increase in air content, as illustrated in Fig. 5. The air content rises approximately linearly with increasing rubber powder dosage. In ordinary concrete, the air content (“air pores” and “solid pores”) is 2.83%. When 5%, 10%, and 20% rubber powder are incorporated, the air content increases to 6.87%, 12.01%, and 15.91%, respectively. This corresponds to a 2.4–5.6-fold increase relative to ordinary concrete, similar to the effect of adding 1%–3% air-entraining agent 31. In rubber powder concrete, “air pores” account for 81.1% (5% rubber powder), 78.4% (10% rubber powder), and 75.5% (15% rubber powder) of the total air content. The “solid pores,” calculated based on the volume ratio of rubber powder to concrete, are 1.3% (5% rubber powder), 2.6% (10% rubber powder), and 3.9% (15% rubber powder), corresponding to 18.9% (XJ5), 21.6% (XJ10),

and 24.5% (XJ15) of the total air content. These results indicate that the proportion of “solid pores” contributed by rubber powder is substantial—approximately one-fifth of the total air content—and increases with higher rubber powder dosages.

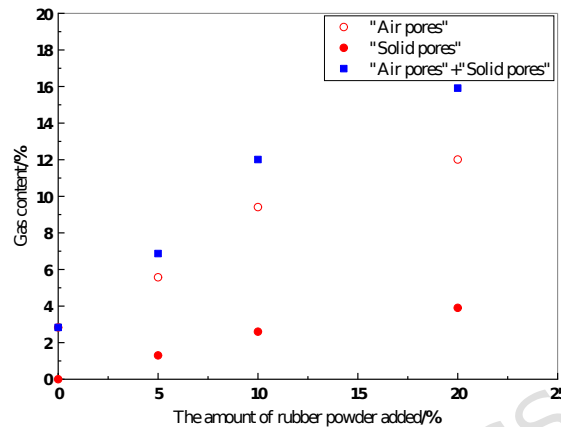


**Fig. 5 Effect of rubber powder on air content of concrete**

For analysis, pore sizes are classified into three intervals: 10–250  $\mu\text{m}$ , 250–350  $\mu\text{m}$ , and 350–1000  $\mu\text{m}$ . The 250  $\mu\text{m}$  threshold corresponds to the diameter of the rubber powder, 350  $\mu\text{m}$  is the maximum pore size beneficial for frost resistance, and 1000  $\mu\text{m}$  approximates the maximum pore size introduced by air-entraining agents. The proportion of pores within each interval relative to the total pore count is used to assess the impact of pore size distribution on frost resistance and the effect of “solid pores.” As shown in Fig. 6, the majority of pores in ordinary concrete (diameter  $>10 \mu\text{m}$ ) are concentrated in the 10–250  $\mu\text{m}$  range, accounting for 91.5% of the total. Pores in the 250–350  $\mu\text{m}$  and 350–1000  $\mu\text{m}$  ranges constitute only 2.1% and 3.8%, respectively. After the addition of rubber powder, larger “air pores” are introduced, increasing the proportion of 350–1000  $\mu\text{m}$  pores to 11.1% (5% rubber powder), 21.1% (10% rubber powder), and 11.7% (15% rubber powder), while the proportion of 10–250  $\mu\text{m}$  pores decreases to 65.2%, 53.3%, and

72.7%, respectively. An increased proportion of 350–1000  $\mu\text{m}$  pores adversely affects both frost resistance and compressive strength.

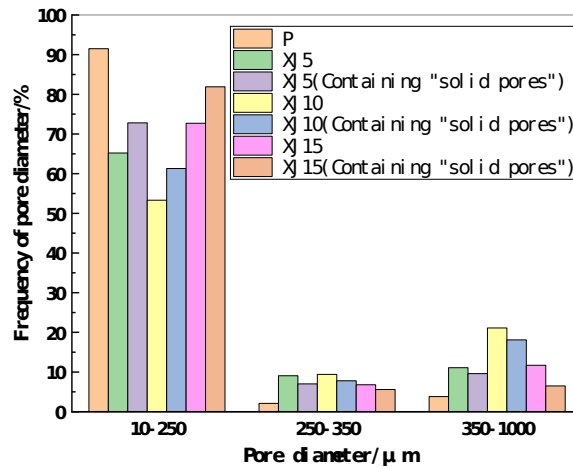


**Fig. 6 Effect of rubber powder on pore size distribution of concrete**

When the “solid pores” introduced by rubber powder are included in the analysis, the proportion of 10–250  $\mu\text{m}$  pores increases by 7.6% (5% rubber powder), 8.0% (10% rubber powder), and 9.2% (15% rubber powder), while the proportion of 350–1000  $\mu\text{m}$  pores decreases by 1.5%, 3.0%, and 5.2%, respectively. These results are comparable to those observed with air-entraining agents [28], indicating that “solid pores” improve the pore size distribution of concrete, and this effect becomes more pronounced with higher rubber powder content. The influence of rubber powder on the content of 250–350  $\mu\text{m}$  pores is minimal, remaining below 10%.

The incorporation of rubber powder introduces a substantial number of “air pores” into the concrete, leading to a nearly linear decrease in the bubble spacing coefficient with increasing rubber powder dosage (as shown Fig. 7). At a 20% rubber powder dosage, the bubble spacing coefficient is reduced to 93  $\mu\text{m}$ , which is comparable to the effect achieved with a 2% dosage of air-entraining agent [32]. It should be noted that, due to test limitations, the bubble

spacing coefficient here only characterizes the spacing between “air pores.” If “solid pores” were included, the bubble spacing coefficient would be even lower; however, this could not be quantified in the present study. Since the square of the bubble spacing coefficient is proportional to the hydrostatic pressure generated by water freezing in capillaries [4], a lower bubble spacing coefficient significantly reduces hydrostatic pressure, thereby mitigating freeze-thaw damage. Therefore, minimizing the bubble spacing coefficient is essential for improving the freeze-thaw durability of concrete.

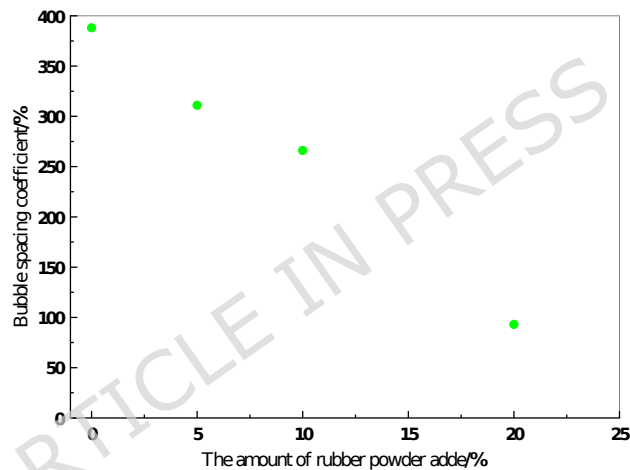


**Fig. 7 Effect of rubber powder on air bubble spacing coefficient of concrete**

The diameter of air bubbles introduced by air-entraining agents ranges from 20  $\mu\text{m}$  to 1000  $\mu\text{m}$ . Test results indicate that the pore sizes introduced by rubber powder are comparable to those produced by air-entraining agents. The primary mechanism by which rubber powder enhances the frost resistance of concrete is the reduction of the bubble spacing coefficient, with “solid pores” playing a particularly beneficial role in optimizing the pore structure.

### **3.2 Influence of nano-silica on pore structure**

As shown in Fig. 8, the air content of XJ10 concrete before the

addition of nano-silica is 12.01%. After incorporating nano-silica, the air content decreases to 6.24% (GXJ5) and 6.07% (GXJ10), corresponding to reductions of 48.0% and 49.5%, respectively. In both GXJ5 and GXJ10, the rubber powder content is maintained at 10%, resulting in a “solid pore” content of 2.6%. This accounts for 41.7% (GXJ5) and 42.8% (GXJ10) of the total air content, which is substantially higher than the proportions observed before the addition of nano-silica (18.9% for XJ5, 21.6% for XJ10, and 24.5% for XJ15). The reduction in air content in GXJ5 and GXJ10 is primarily due to a decrease in “air pores,” which decrease to 3.64% and 3.47%, respectively—values comparable to the air content of ordinary concrete (2.83%).

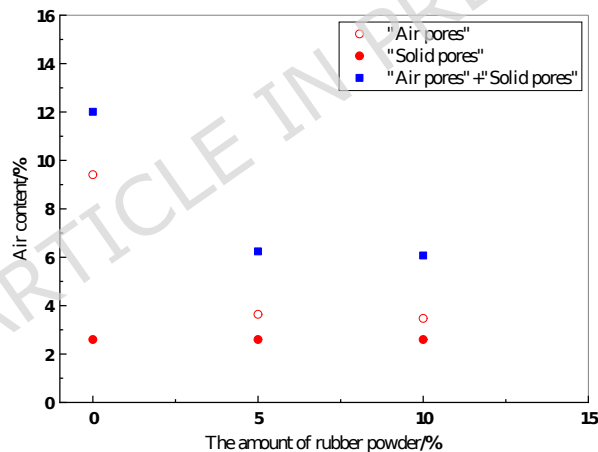


**Fig. 8 Effect of rubber powder on air content of concrete**

Fig. 9 presents the pore size distribution of “air pores” in XJ10 concrete before and after the addition of nano-silica. Prior to nano-silica incorporation, the 10–250  $\mu\text{m}$  pores account for 53.3%, 250–350  $\mu\text{m}$  for 9.4%, and 350–1000  $\mu\text{m}$  for 21.1%. After adding 5% nano-silica, the proportion of 10–250  $\mu\text{m}$  pores increases to 82.5%, while 350–1000  $\mu\text{m}$  pores decrease to 8.9%. With a 10% nano-silica dosage, the 10–250  $\mu\text{m}$  pore proportion further increases to 85.6%, and 350–

1000  $\mu\text{m}$  pores decrease to 5.3%. These results demonstrate that nano-silica reduces the proportion of larger “air pores” and increases that of smaller “air pores.” This effect is attributed to the pozzolanic activity and micro-aggregate filling effect of nano-silica, which fills larger “air pores” and refines the overall pore size distribution. Consequently, the pore structure is optimized, which is beneficial for enhancing the compressive strength of concrete. When “solid pores” are included, the 10–250  $\mu\text{m}$  pore proportion reaches 89.7% (5% nano-silica) and 90.2% (10% nano-silica), values comparable to those of ordinary concrete (91.5%). The presence of rubber powder “solid pores” further increases the proportion of smaller pores, thereby improving the pore size distribution.

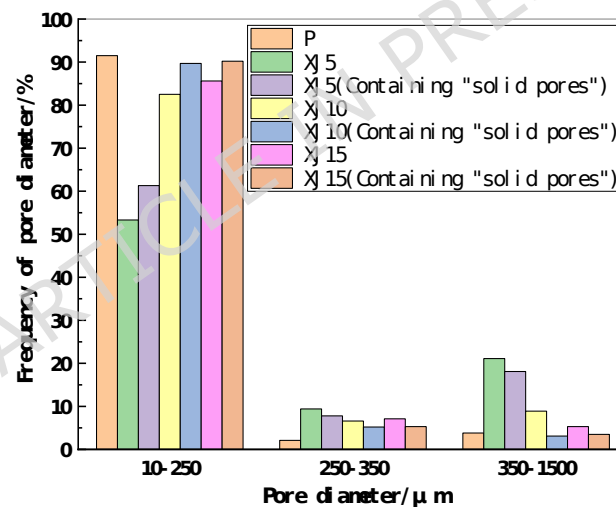


**Fig. 9 Effect of rubber powder on pore size distribution of concrete**

In addition to reducing the overall pore content, nano-silica also decreases the bubble spacing coefficient, as shown in Fig. 10. The coefficient drops from 261  $\mu\text{m}$  (XJ10) to 170  $\mu\text{m}$  (GXJ5, 5% nano-silica) and 182  $\mu\text{m}$  (GXJ10, 10% nano-silica). Notably, all bubble spacing coefficients remain below 250  $\mu\text{m}$ , which is within the favorable range for frost resistance. If “solid pores” are considered,

the bubble spacing coefficient would be further reduced, which is highly beneficial for enhancing the freeze-thaw durability of concrete.

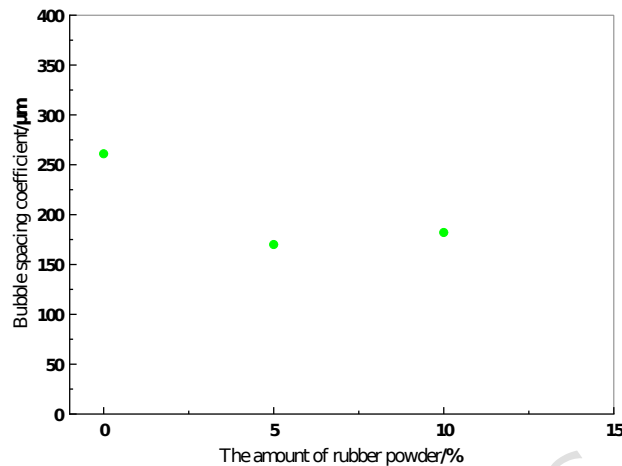


**Fig. 10 The effect of rubber powder on the spacing coefficient of concrete pores**

## 4. Frost resistance of concrete

### 4.1 Compressive strength evolution during freeze-thaw cycles

The combined use of rubber powder and nano-silica markedly improves the frost resistance of concrete, as evidenced by the evolution of compressive strength during freeze-thaw cycles (as shown in Fig. 11). While ordinary concrete exhibits a nearly linear decline in compressive strength, dropping from 34.1 MPa before cycling to 7.6 MPa after 80 cycles—a reduction of 77.7%—the modified concretes (GXJ5 and GXJ10) demonstrate significantly enhanced durability. Prior to freeze-thaw exposure, GXJ5 and GXJ10 achieve compressive strengths of 28.6 MPa and 28.5 MPa, corresponding to 84.4% and 91.5% of that of ordinary concrete, respectively. Remarkably, after 100 freeze-thaw cycles, their compressive strengths remain at 22.4 MPa and 25.4 MPa, representing reductions of only 18.6% and 22.2%. This substantial

improvement highlights the effectiveness of the synergistic modification in mitigating freeze-thaw damage, while maintaining mechanical performance at a level comparable to unmodified concrete. The results demonstrate that the incorporation of rubber powder and nano-silica not only delays the deterioration process but also preserves structural integrity under severe environmental conditions.

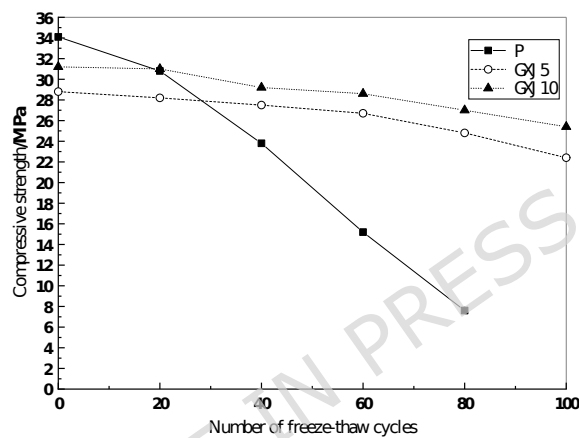


**Fig. 11 Change of compressive strength during freeze-thaw cycle**

#### 4.2 Strength retention rate during freeze-thaw cycles

Concrete is mainly used as a load-bearing material. The retention rate of compressive strength of concrete under harsh conditions can comprehensively reflect the durability of concrete and the safety guarantee as a normal-pressure structure. As shown in Fig. 12, during 20 freeze-thaw cycles, strength of both ordinary concrete and the modified concretes could remain above 90% of their original strength. After 20 freeze-thaw cycles, the strength retention rate of ordinary concrete dropped sharply. At 80 freeze-thaw cycles, the strength retention rate was only 22.3%. In contrast, for the modified concretes, after 80 freeze-thaw cycles, the strength retention rate remained at around 80%. This indicates that the modified concretes

has a high resistance to low temperatures and can meet the durability requirements of concrete in cold regions.

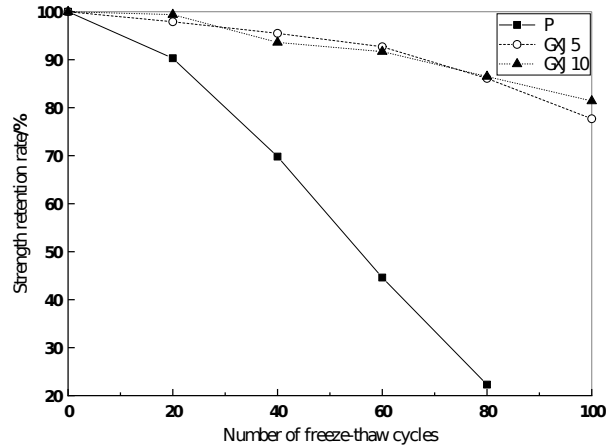


**Fig. 12 Change of strength retention rate during freeze-thaw cycle**

#### 4.3 Pore structure changes during freeze-thaw cycles

The superior frost resistance observed in the modified concretes can be attributed to favorable changes in pore structure during freeze-thaw cycling [as shown in Fig. 13]. Exposure to repeated freezing and thawing typically leads to an increase in pore size, as smaller pores (0–250  $\mu\text{m}$ ) decrease in proportion, while larger pores (250–350  $\mu\text{m}$  and 350–1000  $\mu\text{m}$ ) become more prevalent. However, in concretes containing rubber powder and nano-silica, the reduction in the proportion of 0–250  $\mu\text{m}$  pores is approximately half that of ordinary concrete, and the increases in larger pore fractions are limited to about one-fifth of those seen in the control. This stability in pore size distribution suggests that the “solid pores” introduced by rubber powder are less susceptible to expansion under freezing stress. The inherent elasticity of rubber particles plays a crucial role in absorbing and dissipating stress, thereby reducing crack initiation and propagation during freeze-thaw cycles.

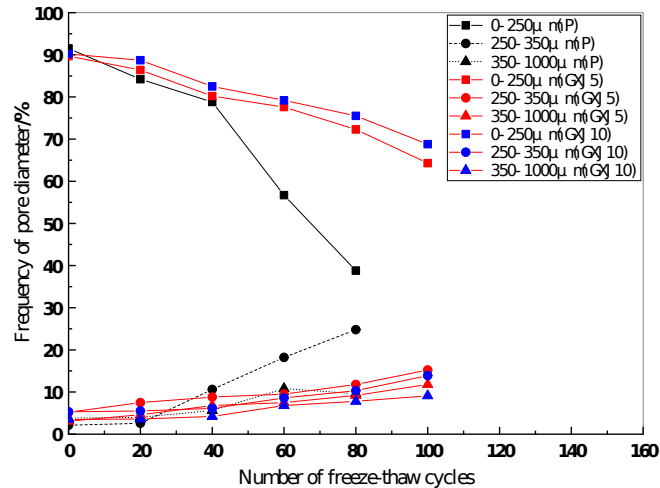


**Fig. 13 Frequency change of concrete pore diameter during freeze-thaw cycle**

Further analysis of the bubble spacing coefficient reinforces these findings—as shown in Fig. 14. Although freeze-thaw cycles generally increase pore diameter and reduce the bubble spacing coefficient, concretes modified with rubber powder and nano-silica experience a much smaller decrease—only one-third to one-half of that observed in ordinary concrete. Maintaining a higher bubble spacing coefficient is beneficial, as it limits the connectivity of pores and impedes the movement of water, thereby reducing the risk of freeze-thaw damage. These results confirm that the tailored pore structure and enhanced stress distribution capacity imparted by rubber powder and nano-silica are key factors in achieving superior frost resistance.

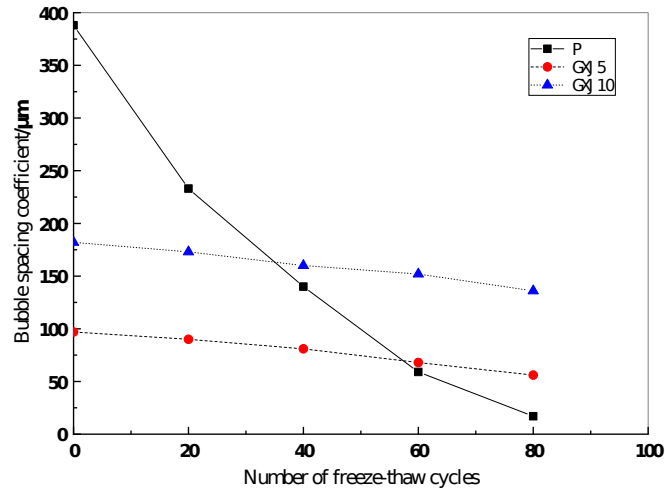


**Fig. 14 Changes of bubble spacing coefficient of concrete during freeze-thaw cycles**

## 5. Discussion

Fig. 15 shows the SEM images of the pore structure of P, XJ15 and GXJ10 respectively, with magnification of 1000 times. It can be seen that compared with P, XJ15 has larger porosity on the whole, but smaller pore size, which is the result of air entraining by rubber powder. The incorporation of rubber particles into P will increase the porosity of P, and rubber particles have the greatest influence on the pore size content of 1000nm<sup>14</sup>. The influence of rubber particles on the gas content of cement mortar can be divided into two effects: first, the rubber particles themselves can be regarded as "solid bubbles", and its pore size is related to the size distribution of rubber particles; Second, rubber particles have air entraining effect, that is, the introduction of "air bubbles".

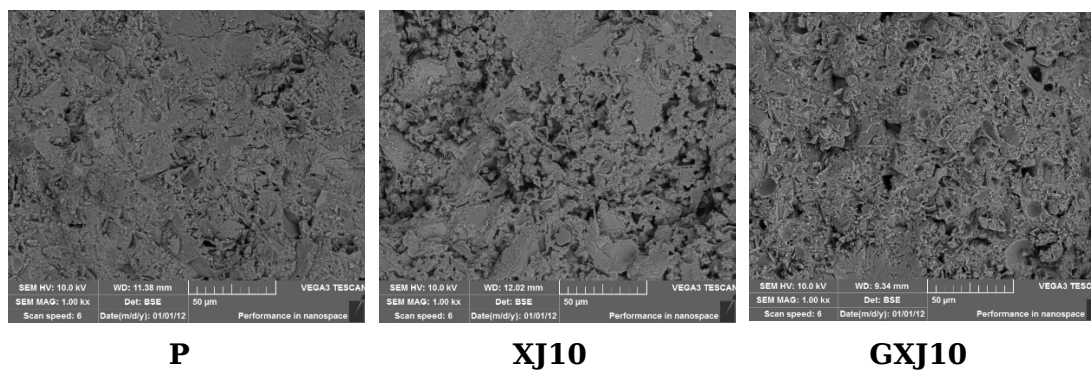


**Fig. 15. Sem image of pore structure of cement mortar**

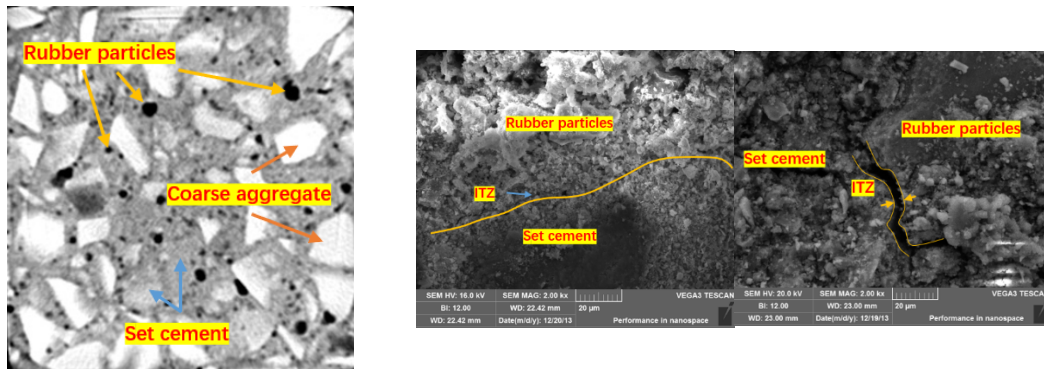
The pore content and pore size of GXJ10 were significantly reduced. The effect of silica powder on XJ15 porosity can also be divided into two effects: First, silica powder can accelerate the hydration reaction process of cement and produce a large amount of C-S-H gel; Second, it can be filled into the pores inside the cement matrix through the filling effect to reduce the porosity. Silica powder mainly reduces the content and size of "air bubbles" in cement mortar, and has no effect on the "solid bubbles" of rubber particles, but can improve the bonding interface between rubber particles and cement matrix, Therefore, silica powder can significantly improve the strength of cement mortar.

The term "solid pore" literally refers to a solid that functions as a pore. Rubber particles in concrete can act as pores due to their elastic modulus and the bonding interface between the rubber particles and the cement paste.

(1) Elastic modulus of rubber particles: The ability of rubber particles to function as pores due to their elastic modulus is relative. The elastic modulus of waste tire rubber is 0.5–2 MPa, approximately tens of thousands of times lower than that of concrete as a whole. When concrete is subjected to external forces and deforms, or when the cement paste undergoes minor deformation due to stress redistribution within the concrete, the rubber particles distributed

in the concrete or cement paste exhibit negligible resistance to deformation. In this regard, the stress behavior of rubber particles is not significantly different from that of real pores.

(2) Bonding interface between rubber particles and cement paste: As shown in Fig.16, from a mesoscopic perspective (Fig.16(a)), rubber particles are relatively uniformly dispersed within the cement paste in concrete, and their distribution as "solid pores" resembles that of real pores. The diameter of the "solid pore" depends on the particle size of the rubber. However, from a microscopic perspective (Fig.16(b)), the "solid pore" includes not only the rubber particle itself but also the bonding interface between the rubber particle and the cement paste, known as the Interfacial Transition Zone (ITZ). Furthermore, the ITZ can be divided into two parts: one is a structurally loose transition zone of cement paste, and the other is a micro-crack between the cement paste and the rubber particle. Due to the limitations of scanning electron microscopy, Figure 14(b) does not clearly show the transition zone of the cement paste, but existing studies have confirmed its existence<sup>33, 34</sup>. The loose structure of the transition zone is attributed to the hydrophobicity of rubber particles, which causes water to accumulate at the interface between the rubber particles and the cement mortar. The water-cement ratio in this region is much higher than that in areas farther from the interface, resulting in coarser C-S-H crystals and a looser structure. Nanoindentation tests indicate that the elastic modulus of the transition zone is only 70% of that of normal cement paste<sup>35</sup>. The micro-cracks between the cement paste and the rubber particles are approximately 20-50  $\mu\text{m}$  wide, caused by volume shrinkage during the curing of the cement mortar. Thus, compared to normally hydrated cement paste, the ITZ exhibits stress resistance behavior that is not significantly different from that of real pores.



(a) Microscopic CT scan image of rubber concrete

(b) Rubber particle - cement stone micro-structural electron microscope image

Fig. 16 Rubber particles as the physical structure of “solid bubbles”

## 6. Conclusion

This study addresses the engineering challenge of air-entraining agent failure in low air pressure environments by proposing the use of rubber powder as a compensatory method. Specifically, rubber powder introduces “solid air pores” to replace traditional “air pores,” leveraging the “air-entraining” effect of rubber powder in combination with the “reinforcing” effect of nano-silica. This coupled approach aims to mitigate severe freeze-thaw damage in concrete subjected to high-altitude, low-pressure, and cold environments. Macro-performance and microstructure tests were conducted to systematically investigate the evolution of concrete pore structure parameters and their influence on frost resistance after freeze-thaw cycling. The main conclusions are as follows:

(1) The incorporation of rubber powder significantly increases the air content of concrete, providing an effect similar to that of air-entraining agents. The “solid pores” account for 18.9% (XJ5), 21.6% (XJ10), and 24.5% (XJ15) of the total air content. As the rubber powder dosage increases, the contribution of “solid pores” to the overall air content also rises. At a 20% dosage, the bubble spacing

coefficient is reduced to 93  $\mu\text{m}$ , which is equivalent to the effect of a 2% air-entraining agent.

(2) The addition of nano-silica to concrete reduces the overall air content, primarily by decreasing the proportion of larger pores (350–1000  $\mu\text{m}$ ). This highlights the contribution of “solid pores” in the 10–250  $\mu\text{m}$  range and ensures that the bubble spacing coefficient remains at a level conducive to enhanced frost resistance.

(3) The synergistic effect of rubber powder and nano-silica results in concrete with slightly lower compressive strength compared to ordinary concrete, but with significantly improved frost resistance. As the number of freeze-thaw cycles increases, the reductions in the proportions of 0–250  $\mu\text{m}$ , 250–350  $\mu\text{m}$ , and 350–1000  $\mu\text{m}$  pores in concrete containing both rubber powder and nano-silica are approximately one-half, one-half, and one-fifth, respectively, of those observed in ordinary concrete. Similarly, the decrease in the bubble spacing coefficient is only about one-third to one-half of that observed in ordinary concrete. These findings demonstrate that concrete modified with rubber powder and nano-silica exhibits superior frost resistance compared to ordinary concrete.

(4) In plateau areas, the supply of cement and aggregates is relatively sufficient, but high-quality fly ash, mineral powder and other admixtures are scarce. The content of nano-silica is low, and the transportation cost is controllable; rubber powder can be recycled from local waste tires, achieving on-site resource utilization. The modified concrete mix ratio used in this paper can be adapted by adjusting the admixtures (such as high-efficiency water reducers), and no additional large equipment is required. Standardized production can be achieved in the construction camp on the plateau by using this method.

## Declarations

**Data Availability Statement:** The datasets used and/or analysed during the current study are available from the corresponding author on reasonable request.

**Funding** □ This study was supported by the National Natural Science Foundation of China (NO. 52179133).

**Acknowledgements** □ Thank my students for their hard work in conducting the experiment.

**Conflicts of Interest:** The authors declare that they have no known competing financial interests or personal relationships that could have appeared to influence the work reported in this paper.

## References

- 1 SU, H. □ Xie, W., Review on frost damages of hydraulic concrete in cold region and Its preventive control, *Bulletin of the Chinese Ceramic Society* (2021) 40(04):1053-1071. (in Chinese).
- 2 Setzer, M.J., Micro-ice-lens formation in porous solid, *Journal of Colloid and Interface Science* (2001) 243:193-201.
- 3 Fagerlund, G., The international cooperative test of the critical degree of saturation method of assessing the freeze/thaw resistance of concrete, *Matériaux et Constructions* (1977) 10:231-253.
- 4 Powers, T.C. □ Willis, T.F., Air requirement of frost-resistant concrete, *Highway Research Board Proceedings* (1950):184-211.
- 5 Powers, T.C. □ Helmuth, R.A., Theory of volume changes in hardened portland cement paste during freezing, *Highway Research Board Proceedings* (1953) 32:285-297.
- 6 Scherer, G.W., Freezing gels, *Journal of Non-Crystalline Solids* (1993) 155:1-25.
- 7 Yuan, J., Wu, Y. □ Zhang, J., Characterization of air voids and frost resistance of concrete based on industrial computerized tomographical technology, *Construction and Building Materials* (2018) 168:975-983.
- 8 Zhang, Y., Zhao, Z., Chen, S. □ Sun, W., Impact of rubber powder on frost resistance of concrete in water and NaCl solution, *Journal of Southeast University (Natural Science Edition)* (2006) (S2):248-252. (in Chinese).
- 9 Richardson, A., Coventry, K., Edmondson, V. □ Dias, E., Crumb rubber used in concrete to provide freeze-thaw protection (optimal particle size), *Journal of Cleaner Production* (2016) 112:599-606.
- 10 Li, X., Influence of atmospheric pressure on performance of air entraining agent

- and air void structures of air-entrained concrete, *Transactions of the Chinese Society of Agricultural Engineering* (2018) 34(24):144-150. (in Chinese).
- 11 Li, Y., Wang, Z. □ Wang, L., Effect of low pressure on bubble generation and development of air entraining agent solution, *Concrete* (2019) (08):144-148. (in Chinese).
  - 12 Sha, H., The compounding and application of air-entraining agents. / Concrete admixtures and their application technologies, *China Civil Engineering Society* (2004):224-226. (in Chinese).
  - 13 Yang, C., Wang, P. □ Sun, M., Experimental study on air content and slump of waste rubber aggregate concrete mixture, *Concrete* (2014) (11):53-55. (in Chinese).
  - 14 Yu, Y. □ Zhu, H., Influences of rubber on drying shrinkage performance of cement based materials, *Acta Materialiae Compositae Sinica* (2017) 34(11):2624-2630. (in Chinese).
  - 15 Grinyš, A., Augonis, A., Daukšys, M. □ Pupeikis, D., Mechanical properties and durability of rubberized and SBR latex modified rubberized concrete, *Construction and Building Materials* (2020) 248.
  - 16 Huang, W., Huang, X., Xing, Q. □ Zhou, Z., Strength reduction factor of crumb rubber as fine aggregate replacement in concrete, *Journal of Building Engineering* (2020) 32(prepublish):101346-101346.
  - 17 Zhang, W., Gong, S. □ Zhang, J., Effect of rubber particles and steel fibers on frost resistance of roller compacted concrete in potassium acetate solution, *Construction and Building Materials* (2018) 187:752-759.
  - 18 Sheng, S., Xiaoyan, H., Aijiu, C., Qing, Z., Zhihao, W. □ Keliang, L., Experimental Analysis and Evaluation of the Compressive Strength of Rubberized Concrete During Freeze-Thaw Cycles, *International Journal of Concrete Structures and Materials* (2023) 17(1).
  - 19 Huang, X., Yue, T., Zhang, J. □ Zhang, J., Experimental Research on the Impact Resistance Mechanical Properties and Damage Mechanism of Rubberized Concrete under Freeze-Thaw Cycling, *Journal of Composites Science* (2024) 8(3):87-.
  - 20 Pham, N.-P., Toumi, A. □ Turatsinze, A., Effect of an enhanced rubber-cement matrix interface on freeze-thaw resistance of the cement-based composite, *Construction and Building Materials* (2019) 207:528-534.
  - 21 Malika, M., Habib, T., Barroso, D.A.J. □ Aissa, A., Durability Properties of Five Years Aged Lightweight Concretes Containing Rubber Aggregates, *Periodica Polytechnica Civil Engineering* (2017) 62(2):386-397.
  - 22 Moustafa, A. □ ElGawady, M.A., Mechanical properties of high strength concrete with scrap tire rubber, *Construction and Building Materials* (2015) 93:249-256.
  - 23 Ma, K., Long, G., Xie, Y., Chen, X. □ Qian, Z., The influence of rubber particles on the performance of self-compacting concrete, *Journal of Silicate Science* (2014) 42(08):966-973.
  - 24 Gupta, T., Sharma, R.K. □ Chaudhary, S., Impact resistance of concrete containing waste rubber fiber and silica fume, *International Journal of Impact*

- Engineering* (2015) 83:76-87.
- 25 Bhatt, K. □ Singh, S., Study on Performance, Durability and Strength of Silica Fume Concrete, *Journal of Progress in Civil Engineering* (2021) 3(8).
- 26 Kansotiya, M., Chaturvedy, G.K. □ Pandey, U.K., Influence of nanosilica and crumbrubberonthe physical and durability characteristics of concrete, *Multiscale and Multidisciplinary Modeling, Experiments and Design* (2024) 7:2877-2892.
- 27 Chaturvedy, G.K., Pandey, U.K. □ Mohan, G., Impact of nano-silica and multi-walled carbon nanotubes on the fire resistance performance of rubberized concrete, *Journal of Building Pathology and Rehabilitation* (2025) 10:161.
- 28 Li, L.G., Zhang, G.-H. □ Kwan, A.K.H., Exploring Submarine 3D Printing: Enhancing Washout Resistance and Strength of 3D Printable Mortar, *American Society of Civil Engineers* (2025) 37(3):04025019.
- 29 Shi, J., Zhao, L., Han, C. □ Han, H., The effects of silanized rubber and nano-SiO<sub>2</sub> on microstructure and frost resistance characteristics of concrete using response surface methodology (RSM), *Construction and Building Materials* (2022).
- 30 SL/T352-2020, Hydraulic Concrete Test Procedure, *Ministry of Water Resources of the People's Republic of China* (2020).
- 31 Jiang, C., Wang, Y., Ouyang, Y., Cai, W., Qian, W. □ Xia, L., Field exposure experiments on the influence of low air pressure environment on the air-void structure of air-entrained concrete and its deterioration mechanism, *Construction and Building Materials* (2024) 453:139067-139067.
- 32 Wawrzeńczyk, J. □ Kowalczyk, H., Estimation of the Spacing Factor Based on Air Pore Distribution Parameters in Air-Entrained Concrete., *Materials (Basel, Switzerland)* (2025) 18(8):1716-1716.
- 33 Momotaz, H., Rahman, M.M., Karim, M.R., Zhuge, Y., Ma, X. □ Levett, P., Properties of the interfacial transition zone in rubberised concrete - an investigation using nano-indentation and EDS analysis *Journal of Building Engineering* (2023) 77:1-17.
- 34 Thomas, B.S., Gupta, R.C., Kalla, P. □ Cseteneyi, L., Strength, abrasion and permeation characteristics of cement concrete containing discarded rubber fine aggregates, *Construction and Building Materials* (2014) 59:204-212.
- 35 Prithvendra Singh, A.M., Devendra Narain Singh, P.D., F., Counto, N.S.N. □ Mhamai, S.R.K., Comprehensive Study of the Properties and Microstructural Characteristics of Rubberized Concrete Using Destructive and Nondestructive Techniques, *Journal of Materials in Civil Engineering* (2025) 37(7):04025207.